Determination of Ocean Mixed Layer Depth from Profile Data

Peter C. Chu and Chenwu Fan

Abstract—**Vertically quasi-uniform layer of temperature (*T*, isothermal layer) and density (ρ, mixed layer) usually exists in upper oceans. The thickness of the mixed layer determines the heat content and mechanical inertia of the layer that directly interacts with the atmosphere. Existing methods for determining mixed layer depth from profile data have large uncertainty. Objective and accurate determination of the mixed layer depth is crucial in ocean dynamics and climate change. This paper describes recently developed optimal linear fitting, maximum angle, and relative gradient methods to determine mixed layer depth from profile data. Profiles from the Global Temperature and Salinity Profile Program (GTSPP) during 1990-2010 are used to demonstrate the capability of these objective methods and to build up global mixed (isothermal) layer depth datasets. Application of the data in climate study is also discussed.**

Key Words—**Mixed layer depth, isothermal depth, difference criterion, gradient criterion, curvature criterion, optimal linear fitting method, maximum angle method, relative gradient method, GTSPP, global mixed layer depth, global isothermal layer depth, barrier layer, compensated layer**

1. Introduction

Transfer of mass, momentum, and energy across the bases of surface isothermal layer and constant-density layer (usually called mixed layer) provides the source for almost all oceanic motions. Underneath the mixed and isothermal layers, there exist layers with strong vertical gradient such as the pycnocline and thermocline. The constant-density (or isothemal) layer depth is an important parameter which largely affects the evolution of the sea surface temperature (SST), and in turn the climate change.

The isothermal layer depth (ILD, H_T) is not necessarily identical to the mixed layer depth (MLD, H_D) due to salinity stratification. There are areas of the World Ocean where H_T is deeper than H_D (Lindstrom et al., 1987; Chu et al., 2002; de Boyer Montegut et al., 2007). The layer difference between H_D and H_T is defined as the barrier layer (BL), which has strong salinity stratification and weak (or neutral) temperature stratification (Fig. 1). The barrier layer thickness (BLT) is often referred to the difference, BLT = H_T - H_D. Less turbulence in the BL

than in the mixed layer due to strong salinity stratification isolates the constant-

density water from cool thermocline water. However, ILD may be thinner than MLD when negative salinity stratification compensates for positive temperature stratification (or the reverse situation) to form a compensated layer (CL) (*Stommel and Fedorov,* 1967; *Weller and Plueddemann,* 1996). The compensated layer thickness (CLT) is defined by   CLT = H_D - H_T. Occurrence of BL and CL affects the ocean heat and salt budgets and the heat exchange with the atmosphere, and in turn influences the climate change.

Objective and accurate identification of H_T and H_D is the key to successfully determining the BL or CL. However, three existing types of criteria (on the base of difference, gradient, and curvature) to determine H_T and H_D are either subjective or inaccurate. The difference criterion requires the deviation of T (or ρ) from its near surface (i.e., reference level) value to be smaller than a certain fixed value. The gradient criterion requires $\partial T/ \partial z$ (or $\partial \rho/ \partial z$) to be smaller than a certain fixed value. The curvature criterion requires $\partial^2 T/ \partial z^2$ (or $\partial^2 \rho/\partial z^2$) to be maximum at the base of mixed layer ($z =$ -H_D). Obviously, the difference and gradient criteria are subjective. For example, the criterion for determining H_T for temperature varies from 0.8^{o}C (Kara et al., 2000), 0.5^{o}C (Wyrtki, 1964) to 0.2^{o}C (de Boyer Montegut et al., 2007). The reference level changes from near surface (Wyrtki, 1964) to 10 m depth (de Boyer Montegut et al., 2007). Defant (1961) was among the first to use the gradient method. He uses a gradient of 0.015^{o}C/m to determine H_T for temperature of the Atlantic Ocean; while Lukas and Lindstrom (1991) used 0.025^{o}C/m. The curvature criterion is an objective method (Chu et al, 1997, 1999, 2000; Lorbacher et al., 2006); but is hard to use for profile data with noise (even small), which will be explained in Section 5. Thus, it is urgent to develop a simple objective method for determining mixed layer depth with capability of handling noisy data.

In this study, we use several recently developed objective methods to establish global (H_D, H_T) dataset from the Global Temperature and Salinity Profile Program (GTSPP) during 1990-2010. The quality indices for these methods are approximately 96% (100% for perfect determination). The results demonstrate the existence and variability of (BL, CL).

The outline of this paper is as follows. Section 2 describes the GTSPP data. Section 3 shows the large uncertainty of the existing methods. Section 4 presents the methodology. Section 5 shows the comparison to the existing objective method (i.e., the curvature method). Section 6 presents the quality index for validation. Section 7 shows the global (H_D, H_T) dataset calculated from the GTSPP profile data (1990-2010). In Section 8 we present the conclusions.

2. GTSPP

The following information was obtained from the website of the International Oceanographic Commission of UNESCO (IODE) http://www.iode.org/. GTSPP is a cooperative international project. It seeks to develop and maintain a global ocean Temperature-Salinity resource with data that are both up-to-date and of the highest quality possible. Making global measurements of ocean temperature and salinity (T-S) quickly and easily accessible to users is the primary goal of the GTSPP. Both real-time data transmitted over the Global Telecommunications System (GTS), and delayed-mode data received by the NODC are acquired and incorporated into a continuously managed database. Countries contributing to the project are Australia, Canada, France, Germany, Japan, Russia, and the United States. Canada's Marine Environmental Data Service (MEDS) leads the project, and has the operational responsibility to gather and process the real-time data. MEDS accumulates real-time data from several sources via the GTS. They check the data for several types of errors, and remove duplicate copies of the same observation before passing the data on to NODC. The quality control procedures used in GTSPP were developed by MEDS, who also coordinated the publication of those procedures through the Intergovernmental Oceanographic Commission (IOC).

The GTSPP handles all temperature and salinity profile data. This includes observations collected using water samplers, continuous profiling instruments such as CTDs, thermistor chain data and observations acquired using thermosalinographs. These data will reach data processing centres of the Program through the real-time channels of the IGOSS program or in delayed mode through the IODE system. Real-time data in GTSPP are acquired from the Global Telecommunications System in the bathythermal (BATHY) and temperature, salinity & current （TESAC) codes forms supported by the WMO. Delayed mode data are contributed directly by member states of IOC (Sun, 2008). Fig. 1 shows increasing of observational stations especially the TESAC due to input of Argo floats (Fig. 2).

The GTSPP went through quality control procedures that make extensive use of flags to indicate data quality. To make full use of this effort, participants of the GTSPP have agreed that data access based on quality flags will be available. That is, GTSPP participants will permit the selection of data from their archives based on quality flags as well as other criteria. These flags are always included with any data transfers that take place. Because the flags are always included, and because of the policy regarding changes to data, as described later, a user can expect the participants to disseminate data at any stage of processing. Furthermore, GTSPP participants have agreed to retain copies of the data as originally received and to make these available to the user if requested (GTSPP Working Group, 2010).
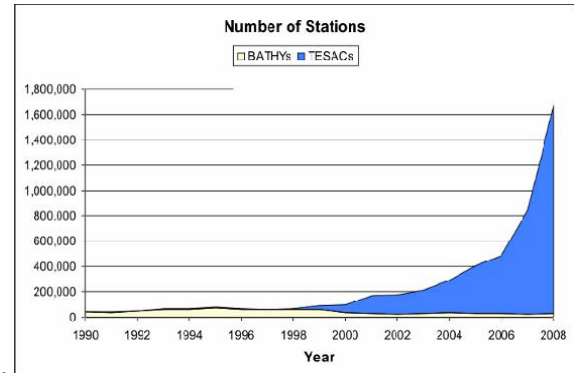

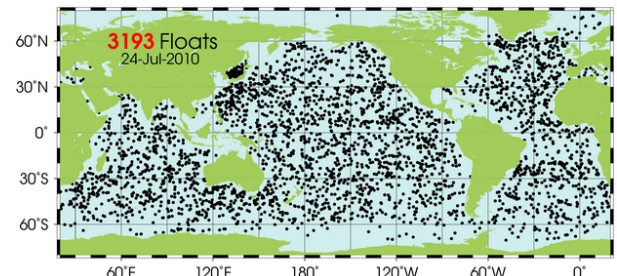**Fig. 1. The number of stations reported as BATHYs and TESACs (from Sun, 2008).**

Fig. 2. World-wide distribution of Argo floats (from the website: http://www.argo.ucsd.edu/).

3. Large Uncertainty of the Existing Methods

As pointed in the introduction section, the criteria for the difference and gradient methods are subjective. For the difference method, the criterion changes from 0.2^oC (Thompson, 1976, Crieterion-1) for the North Pacific, 0.5^oC (Wyrtki, 1964; Obata et al., 1996, Crieterion-2) for the global oceans, 0.8^oC (Kara et al., 2000, Crieterion-3) for the global oceans, to 1.0^oC (Rao et al., 1989, Crieterion-4) for the Indian Ocean. Four datasets of mixed layer depth were obtained from the GTSPP temperature profiles using these criteria. The probability density functions (PDF) for the four datasets (Fig. 3) show large difference. The root-mean square difference (RMSD) between Criterion-i and Criterion-j is calculated by

$$\text{RMSD}(i, j) = \sqrt{\frac{1}{N} \sum_{n=1}^{N} \left(h_n^{(i)} - h_n^{(j)} \right)^2} \ .$$

The relative RMSD (RRMSD) between Criterion-i and Criterion-j is calculated by

$$\text{RRMSD}(i, j) = 2 * \text{RMSD}(i, j) / (\overline{H}_T^{(i)} + \overline{H}_T^{(j)}) \ ,$$

where $\overline{H}_T^{(i)}$ and $\overline{H}_T^{(j)}$ are the mean isothermal layer depth using Criterion-i and Criterion-j. The RMSD has a minimum value of 43 m between Criterion-2 (0.5°C) and Criterion-3 (0.8°C) and a maximum value of 109 m between Criterion-1 (0.2°C) and Criterion-4 (1.0°C). Such a large uncertainty makes the difference method less credible in determine the mixed layer depth from the profile data.

Similarly, the gradient method also uses various criterion such as 0.015°C/m (Defant, 1961) and 0.025°C/m (Lukas and Lindstrom, 1991). The RMSD between the two is around 70 m.
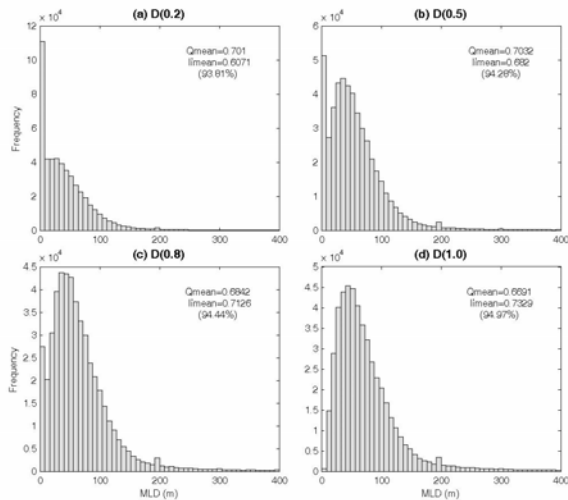
Fig. 1. PDF of the isothermal depth determined by the difference method using different criterion: (a) 0.2°C, (b) 0.5°C, (c) 0.8°C, and (d) 1.0°C.

Table-1. RMSD and RRMSD between two different criterion using the difference method.

Between Criteria	RMSD (m)	RRMSD
(1,2)	51	0.82
(1,3)	74	1.09
(1,4)	109	1.49
(2,3)	43	0.57
(2,4)	88	1.08
(3,4)	71	0.81

4. Recently Developed Objective Determination of MLD and ILD

Recently, Chu and Fan (2010a, b) developed several objective methods for identify (H_D, H_T): optimal linear fitting, maximum angle, and relative gradient. Among them, the first two methods are used for analyzing high (less than 5 m) resolution profiles and the third one is suitable for analyzing low (greater than 5 m) resolution profiles.

4.1. Optimal Linear Fitting (OLF) Method

We use temperature profile as example for illustration. For detailed information, please see Chu and Fan (2010a). Assume a temperature profile which can be represented by $[T(z_i)]$. A linear polynomial is used to fit the profile data from the first point near the surface (z_1) to a depth, z_k (marked by a circle in Fig. 3). The original and fitted data are represented by (T_1, T_2, …, T_k) and ($\hat{T}_1, \hat{T}_2, ..., \hat{T}_k$), respectively. The root-mean square error E_1 is calculated by

$$E_1(k) = \sqrt{\frac{1}{k} \sum_{i=1}^{k} (T_i - \hat{T}_i)^2} \ . \tag{1}$$

The next step is to select n data points ($n << k$) from the depth z_k downward: T_{k+1}, T_{k+2}…, T_{k+n}. A small number n is used because below the mixed layer temperature has large vertical gradient and because our purpose is to identify if z_k is at the mixed layer depth. The linear polynomial for data points (z_1, z_2, …, z_k) is extrapolated into the depths (z_{k+1}, z_{k+2}, …, z_{k+n}): $\hat{T}_{k+1}, \hat{T}_{k+2}, ..., \hat{T}_{k+n}$. The bias of the linear fitting for the n points is calculated by

$$\text{Bias}(k) = \frac{1}{n} \sum_{j=1}^{n} (T_{k+j} - \hat{T}_{k+j}) \ . \tag{2}$$
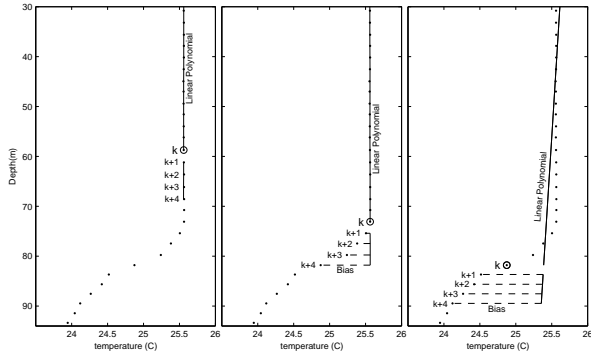
If the depth z_k is inside the mixed layer (Fig. 3a), the linear polynomial fitting is well representative for the data points (z_1, z_2, …, z_{k+n}). The absolute value of the bias,

$$E_2(k)= |\text{Bias}(k)|, \tag{3}$$

for the lowest n points are usually smaller than E_1 since differences between observed and fitted data for the lowest n points may cancel each other. If the depth z_k is located at the base of the mixed layer, $E_2(k)$ is large and $E_1(k)$ is small (Fig. 3b). If the depth z_k is located below at the base of the mixed layer (Fig. 3c), both $E_1(k)$ and $E_2(k)$ are large. Thus, the criterion for determining the mixed layer depth can be described as

$$\frac{E_2(z_k)}{E_1(z_k)} \to \max, \quad H_T = -z_k \ , \tag{4}$$

which is called the optimal linear fitting (OLF) method. The OLF method is based on the notion that there exists a near-surface quasi-homogeneous layer in which the standard deviation of the property (temperature, salinity, or density) about its vertical mean is close to zero. Below the depth of H_T, the property variance should increase rapidly about the vertical mean.

Fig. 3. Illustration of the optimal linear fitting (OLF) method: (a) z_k is inside the mixed layer (small E_1 and E_2), (b) z_k at the mixed layer depth (small E_1 and large E_2), and (c) z_k below the mixed layer depth (large E_1 and E_2) (after Chu and Fan, 2010a).

4.2. Maximum Angle Method

We use density profile as example for illustration. Let density profiles be represented by $[\rho(z_k)]$. The density profile is taken for illustration of the new methodology. A first vector ($\mathbf{A}_1$, downward positive) is constructed with linear polynomial fitting of the profile data from z_{k-m} to a depth, z_k (marked by a circle in Fig. 4) (m < k). A second vector ($\mathbf{A}_2$, pointing downward also) from one point below that depth (i.e., z_{k+1}) is constructed to a deeper level with the same number of observational points as the first vector (i.e., from z_{k+1} to z_{k+m}). The dual-linear fitting can be represented by

$$\rho(z) = \left\{ \begin{array}{ll} c_k^{(1)} + G_k^{(1)} z, & z = z_{k-m}, z_{k-m+1}, \ldots z_k \\ c_k^{(2)} + G_k^{(2)} z, & z = z_{k+1}, \ldots z_{k+m} \end{array} \right. , \quad (5)$$

where $c_k^{(1)}$, $c_k^{(2)}$, $G_k^{(1)}$, $G_k^{(2)}$ are the fitting coefficients. For high resolution (around 1 m), we set

$$m = \left\{ \begin{array}{ll} 10, & \text{for } k > 10 \\ k - 1, & \text{for } k \leq 10 \end{array} \right. . \quad (6)$$

Since the vertical gradient has great change at the constant-density (isothermal) layer depth, the angle θ_k reaches its maximum value if the chosen depth (z_k) is the mixed layer depth (see Fig. 4a), and smaller if the chosen depth z_k is inside (Fig. 4b) or outside (Fig. 4c) of the mixed layer. Thus, the maximum angle principle can be

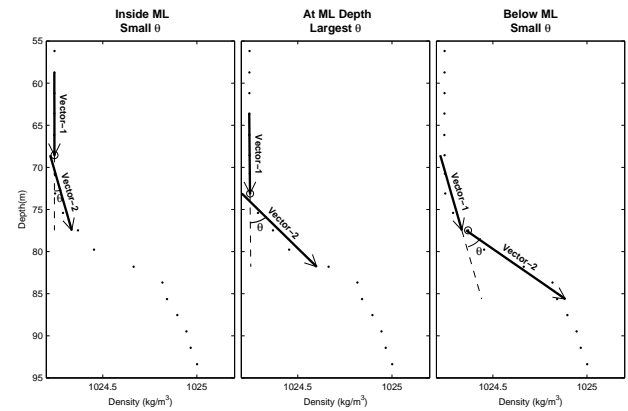used as optimization to determine the mixed (or isothermal) layer depth,

$$\theta_k \to \max, \quad H_D = -z_k .$$

In practical, the angle θ_k is hard to calculate. We use tan θ_k instead, i.e.,

$$\tan \theta_k \to \max, \quad H_D = -z_k . \quad (7)$$

With the given fitting coefficients $G_k^{(1)}$, $G_k^{(2)}$, the value of tan θ_k can be easily calculated by

$$\tan \theta_k = \frac{G_k^{(2)} - G_k^{(1)}}{1 + G_k^{(1)} G_k^{(2)}} . \quad (8)$$

Fig. 4. Illustration of the method: (a) z_k is inside the mixed layer (small θ), (b) z_k at the mixed layer depth (largest θ), and (c) z_k below the mixed layer depth (small θ) (after Chu and Fan, 2010b).

5. Comparison to the Existing Objective Method

The existing objective method is the curvature criterion, which requires $\partial^2 T / \partial z^2$ (or $\partial^2 \rho / \partial z^2$) to be minimum (maximum) at the base of mixed layer. We compare the maximum angle method to the curvature method as an example. To illustrate the superiority of the recently developed methods, an analytical temperature profile with ILD of 20 m is constructed by

$$T(z) = \left\{ \begin{array}{ll} 21^o C, & -20 \text{ m} < z \leq 0 \text{ m} \\ 21^o C + 0.25^o C \times (z + 20 \text{ m}), & -40 \text{ m} < z \leq -20 \text{ m} \\ 7^o C + 9^o C \times \exp\left(\dfrac{z + 40 \text{ m}}{50 \text{ m}}\right), & -100 \text{ m} \leq z \leq -40 \text{ m}. \end{array} \right.$$

$$(9)$$

This profile was discretized with vertical resolution of 1 m from the surface to 10 m depth and of 5 m below 10 m depth. The discrete profile was smoothed by 5-point moving average in order to remove the sharp change of the gradient at 20 m and 40 m depths. The smoothed profile data [$T(z_k)$] is shown in Fig. 5a.

The second-order derivatives of $T(z_k)$ versus depth is computed by nonhomogeneous mesh difference scheme,

$$\frac{\partial^2 T}{\partial z^2}\Big|_{z_k} \approx \frac{1}{z_{k+1} - z_{k-1}} \left(\frac{T_{k+1} - T_k}{z_{k+1} - z_k} - \frac{T_k - T_{k-1}}{z_k - z_{k-1}} \right), \qquad (10)$$

Here, $k = 1$ refers to the surface, with increasing values indicating downward extension of the measurement. Eq.(10) shows that we need two neighboring values, T_{k-1} and T_{k+1}, to compute the second-order derivative at z_k. For the surface and 100 m depth, we use the next point value, that is,

$$\frac{\partial^2 T}{\partial z^2}\Big|_{z=0} = \frac{\partial^2 T}{\partial z^2}\Big|_{z=-1 \text{ m}}, \quad \frac{\partial^2 T}{\partial z^2}\Big|_{z=-100 \text{ m}} = \frac{\partial^2 T}{\partial z^2}\Big|_{z=-95 \text{ m}} . \quad (11)$$

Fig. 5b shows the calculated second-order derivatives from the profile data shown in Fig. 5a. Similarly, $\tan \theta_k$ is calculated using Eq.(8) for the same data profile (Fig. 5c). For the profile data without noise, both curvature method (i.e., depth with minimum $\partial^2 T/\partial z^2$, see Fig. 5b) and maximum angle method [i.e., depth with max ($\tan \theta$), see Fig. 5c)] have the capability to identify the ILD, i.e., $H_T = 20$ m.
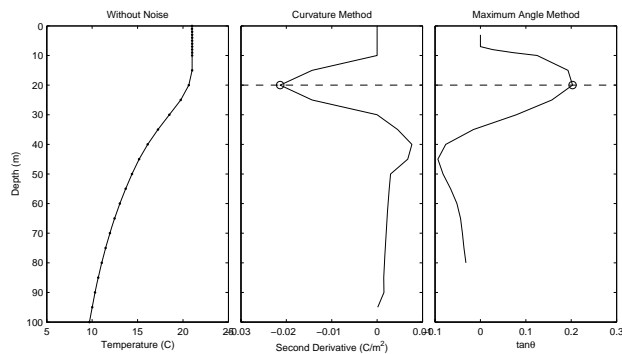

Fig. 5. (a) Smoothed analytic temperature profile (6) by 5-point moving average, calculated (b) ($\partial^2 T/\partial z^2)_k$, and (c) ($\tan \theta)_k$ from the profile data (Fig. 5a). At 20 m depth, ($\partial^2 T/\partial z^2)_k$ has a minimum value, and ($\tan \theta)_k$ has a maximum value (after Chu and Fan 2010b).

Random noises with mean of zero and standard deviation of 0.02°C (generated by MATLAB) are added to the original profile data at each depth for 1000 times. After this process, 1000 sets of temperature profiles were produced. Among them, one temperature profile data is shown in Fig.6a. For this particular profile, the second-order derivatives ($\partial^2 T/\partial z^2$) and $\tan \theta$ were calculated at

each depth. The isothermal depth is 9 m (error of 11 m) using the curvature method (Fig. 6b) and 20 m (no error) using the maximum angle method. Usually, the curvature method requires smoothing for noisy data (Chu, 1999; Lorbacher et al., 2006). To evaluate the usefulness of smoothing, a 5-point moving average was applied to the 1000 "contaminated" profile data. For the profile data (Fig. 6a) after smoothing, the second derivatives were calculated for each depth (Fig. 6c). The isothermal depth was identified as 8 m. Performance for the curvature method (with and without smoothing) and the maximum angle method is determined by the relative root-mean square error (RRMSE),

$$\text{RRMSE} = \frac{1}{H_T^{ac}} \sqrt{\frac{1}{N} \sum_{i=1}^{N} (H_T^{(i)} - H_T^{ac})^2} , \qquad (12)$$

where H_T^{ac} (= 20 m) is the ILD for the original temperature profile (Fig. 7a); N (= 1000) is the number of "contaminated" profiles; and $H_T^{(i)}$ is the calculated ILD for the i-th profile. Without 5-point moving average, the curvature method identified only 6 profiles (out of 1000 profiles) with ILD of 20 m, and the rest profiles with ILDs ranging relatively evenly from 1 m to 10 m. The RRMSE is 76%. With 5-point moving average, the curvature method identified 413 profiles with ILD of 20 m, 164 profiles with ILD of 15 m, 3 profiles with ILD of 10 m, and the rest profiles with ILDs ranging relatively evenly from 2 m to 8 m. The RRMSE is 50%. However, without 5-point moving average, the maximum angle method identified 987 profiles with ILD of 20 m, and 13 profiles with ILD of 15 m. The RRMSE is less than 3%.
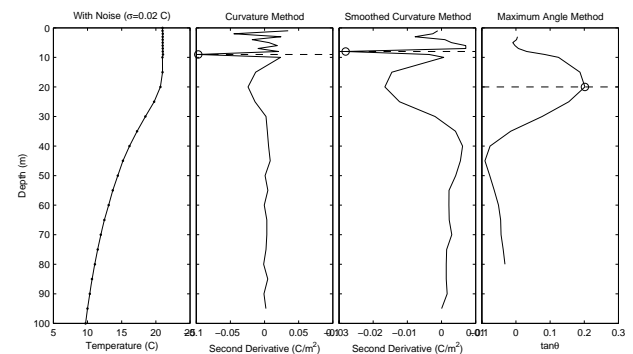
Fig. 6. One out of 1000 realizations: (a) temperature profile shown in Fig. 7a contaminated by random noise with mean of zero and standard deviation of 0.02°C, (b) calculated ($\partial^2 T/\partial z^2)_k$ from the profile data (Fig. 8a) without smoothing, (c) calculated ($\partial^2 T/\partial z^2)_k$ from the smoothed profile data (Fig. 6a) with 5-point moving average, and (d) calculated ($\tan \theta)_k$ from the profile data (Fig. 6a) without smoothing (after Chu and Fan, 2010b).

6. Quality Index for Validation

Lorbacher et al. (2006) proposed a quality index (QI) for determining H_D (similar for H_T),

$$QI = 1 - \frac{\mathrm{rmsd}\left(\rho_k - \hat{\rho}_k\right)|_{(H_1, H_D)}}{\mathrm{rmsd}\left(\rho_k - \hat{\rho}_k\right)|_{(H_1, 1.5 \times H_D)}}, \qquad (13)$$

which is one minus the ratio of the root-mean square difference (rmsd) between the observed to fitted temperature in the depth range from the surface to H_D to that in the depth of $1.5 \times H_D$. H_D is well defined if QI > 0.8; can be determined with uncertainty for QI in the range of 0.5-0.8; and can't be identified for QI < 0.5. For the curvature criterion, QI above 0.7 for 70% of the profile data, including conductivity-temperature-depth and expendable bathythermograph data obtained during World Ocean Circulation Experiment (Lorbacher et al., 2006).

7. Global (H_D, H_T) Dataset

The global (H_D, H_T) dataset has been established from the GTSPP (T, S) profiles using the recently developed objective methods (optimal linear fitting, maximum angle, and relative gradient). The quality index (QI) is computed for each profile using (13). To show the seasonal variability, the global (H_D, H_T) data were binned by month and averaged in $2^\circ \times 2^\circ$ grid cells. The overall value of the quality index is around 0.95 (Figs. 7-12) much higher than the curvature method reported by Lorbacher et al. (2006).

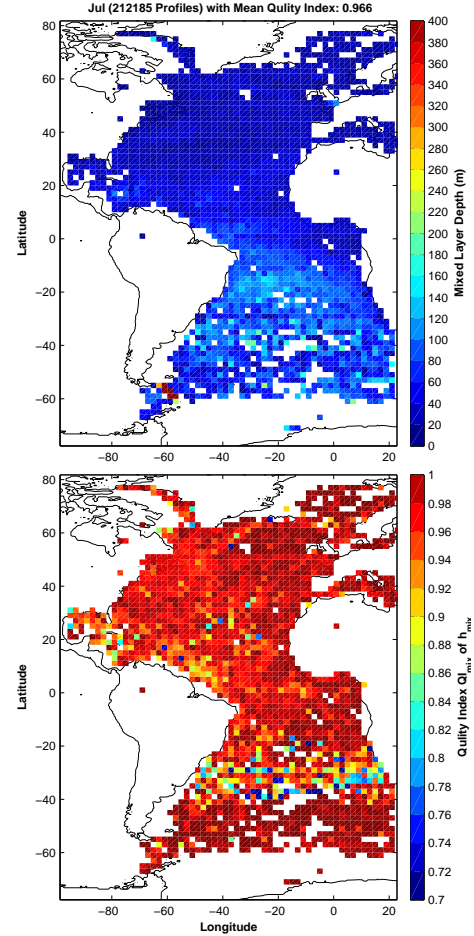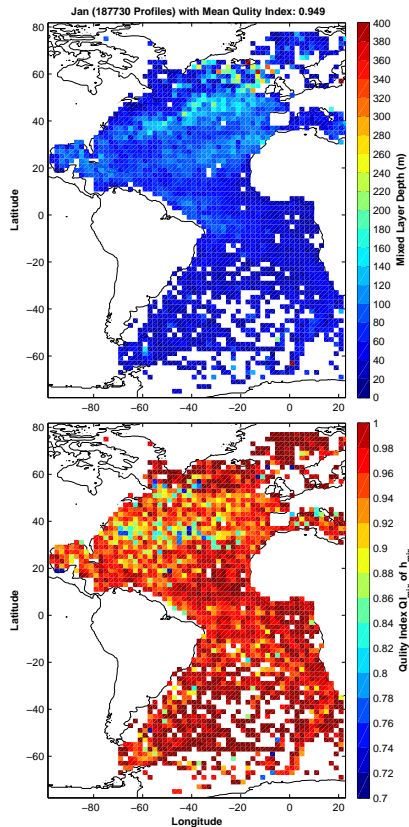**Fig. 7. Atlantic Ocean (January): (a) calculated isothermal layer depth (m), and (b) quality index.**

Fig. 8. Atlantic Ocean (July): (a) calculated isothermal layer depth (m), and (b) quality index.
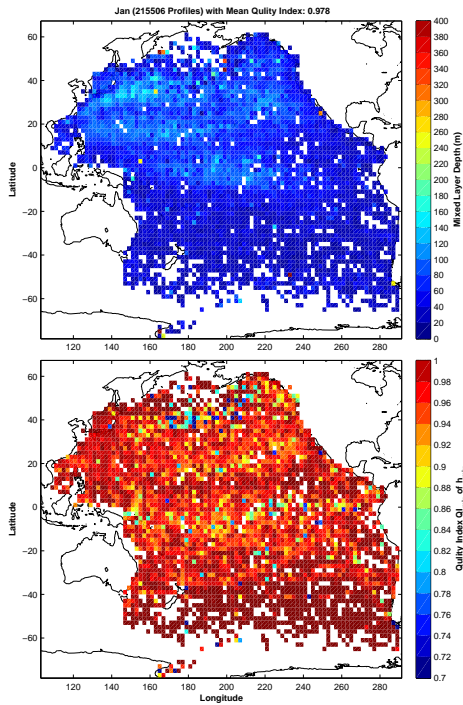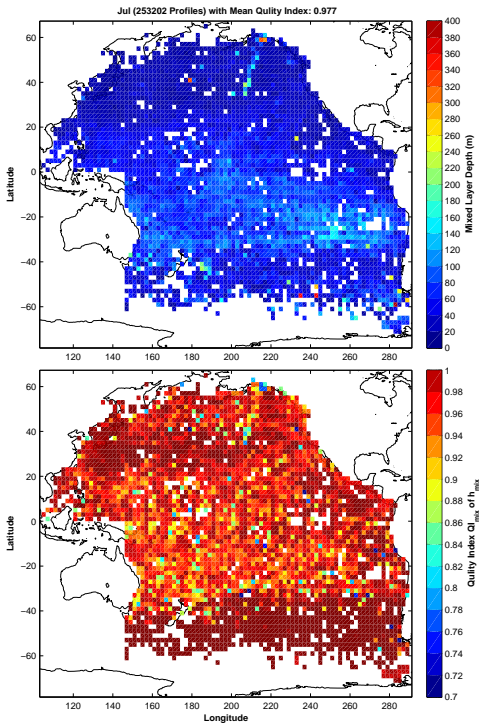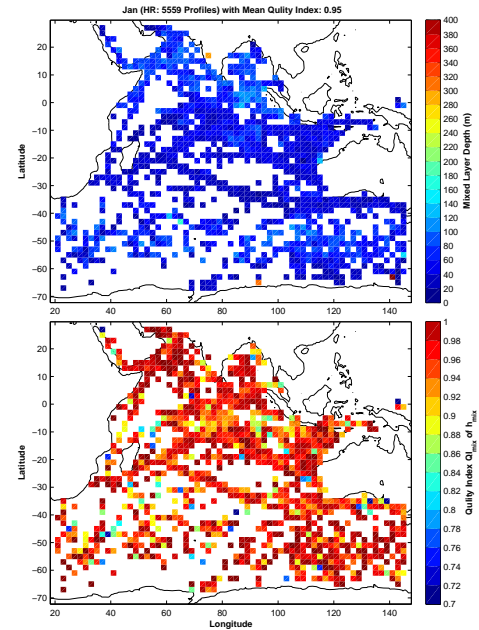
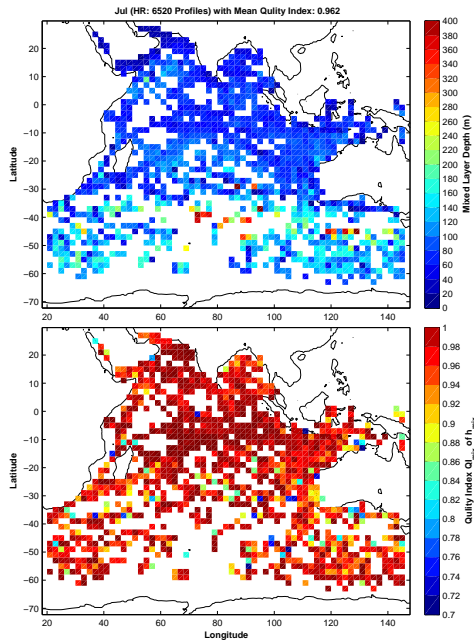**Fig. 9. Pacific Ocean (January): (a) calculated isothermal layer depth (m), and (b) quality index.**

Fig. 10. Pacific Ocean (July): (a) calculated isothermal layer depth (m), and (b) quality index.

8. Conclusions

In this paper, we established global mixed (isothermal) layer data set using recently developed objective methods with high quality indices (optimal linear fitting, maximum angle). Several advantages of this approach

are listed as follows: (a) Procedure is totally objective without any initial guess (no iteration); and (b) No any differentiations (first or second) are calculated for the profile data. The calculated (H_D, H_T) are ready to use for various studies such as the global distribution of barrier and compensated layers, heat content in the surface isothermal layer (heat source for exchange with the atmosphere), and impact on climate change.

Fig. 11. Indian Ocean (January): (a) calculated isothermal layer depth (m), and (b) quality index.

Fig. 12. Indian Ocean (July): (a) calculated isothermal layer depth (m), and (b) quality index.

References

Chu, P.C., 1993: Generation of low frequency unstable modes in a coupled equatorial troposphere and ocean mixed layer. *J. Atmos. Sci.*, **50**, 731-749.

Chu, P.C., 2006: *P-Vector Inverse Method*. Springer, Berlin, 605 pp.

Chu, P.C., C.R. Fralick, S.D. Haeger, and M.J. Carron, 1997: A parametric model for Yellow Sea thermal variability. *J. Geophys. Res*., **102**, 10499-10508.

Chu, P.C., Q.Q. Wang, and R.H. Bourke, 1999: A geometric model for Beaufort/Chukchi Sea thermohaline structure. *J. Atmos. Oceanic Technol*., **16**, 613-632.

Chu, P.C., C.W. Fan, and W.T. Liu, 2000: Determination of sub-surface thermal structure from sea surface temperature. *J. Atmos. Oceanic Technol.*, **17**, 971-979.

Chu, P.C., Q.Y. Liu, Y.L. Jia, C.W. Fan, 2002: Evidence of barrier layer in the Sulu and Celebes Seas. *J. Phys. Oceanogr*., **32**, 3299-3309.

Chu, P.C., and C.W. Fan, 2010a: Optimal linear fitting for objective determination of ocean mixed layer depth from glider profiles. *J. Atmos. Oceanic Technol*., acceptance subject to minor revision.

Chu, P.C., and C.W. Fan, 2010b: Barrier layer near the East Florida Coast in winter detected from Seaglider data with maximum angle method. *J. Mar Syst.*, submitted.

de Boyer Montegut, Mignot, C., ,J., Lazar, A., Cravatte, C., 2007. Control of salinity on the mixed layer depth in the world ocean: 1. General description. J. Geophys. Res., 112, C06011, doi: 10.1029/2006JC003953.

Defant, A., 1961: Physical Oceanography, Vol 1, 729 pp., Pergamon, New York.

GTSPP Workin Group, 2010: GTSPP Real-Time Quality Control Manual. IOC Manual and Guides 22, pp. 148.

Kara, A. B., P.A. Rochford, and H. E. Hurlburt, 2000: Mixed layer depth variability and barrier layer formation over the north Pacific Ocean. *J. Geophys. Res*., **105**, 16783-16801.

Lindstrom, E., R. Lukas, R. Fine, E. Firing, S. Godfrey, G. Meyeyers, and M. Tsuchiya, 1987: The western Equatorial Pacific ocean circulation study. *Nature*, **330**, 533-537.

Lorbacher, K., Dommenget, D., Niiler, P.P., Kohl, A. 2006. Ocean mixed layer depth: A subsurface proxy of ocean-atmosphere variability. J. Geophys. Res., 11, C07010, doi:10.1029/2003JC002157.

Lukas and Lindstrom, 1991: The mixed layer of the western equatorial Pacific Ocean. *J. Geophys. Res*., **96**, 3343-3357.

Sun, L.C., 2008: GTSPP Bi-Annual Report for 2007 – 2008. pp.14. The document can be downloaded from: http://www.nodc.noaa.gov/GTSPP/document/reports/GTSPPReport2007-2008V2.pdf.

Wyrtki, K., 1964. The thermal structure of the eastern Pacific Ocean. *Dstch. Hydrogr. Zeit., Suppl. Ser. A*, **8**, 6-84.